Articles

First-Principles Investigation of Enantioselective Catalysis: Asymmetric Allylic Amination with Pd Complexes Bearing P,N-Ligands

Peter E. Blöchl*,† and Antonio Togni‡

Zurich Research Laboratory, IBM Research Division, CH-8803 Rüschlikon, Switzerland, and Laboratory for Inorganic Chemistry, Swiss Federal Institute of Technology, ETH Zentrum, CH-8092 Zurich, Switzerland

Received May 21, 1996⊗

Site selectivity for nucleophilic attack of a π-allyl−Pd(II) complex with a bidentate phosphine−pyrazole ligand by an amine has been investigated with first-principles density functional calculations using the projector augmented wave method. The interplay between steric and electronic effects, namely the trans influence, is elucidated. While the trans influence favors nucleophilic attack at the carbon in a pseudo-trans position to the phosphine, site selectivity is dominated by steric effects between the allyl group and a groove in the catalyst surface, which prescribe an orientation of the allyl out of the P−Pd−N plane. The direction of this out-of-plane orientation determines the site of nucleophilic attack for a given isomer of the allyl complex, irrespective of whether this site is cis or trans to the phosphine. Our results provide insight into the observed relation between isomeric distributions of the allyl complexes and the resulting selectivities.

1. Introduction

Molecular recognition in biological systems is sensitive to chirality. Access to a pool of molecules with well-defined handedness, from which more complex chemicals can be obtained using standard synthesis techniques, is therefore of utmost importance to the pharmaceutical, agrochemical, and fragrance industries. Organometallic catalysis is one important route to obtain asymmetric products with high purity.[1] A detailed understanding of the reaction mechanism is a prerequisite for efficiently directing the molecular engineering of new catalytic systems and processes. While experiments provide many important clues, they have their limitations. Asymmetric catalysis is a challenge to theoretical investigations, on the one hand because it is sensitive to small energy differences of a few kilojoules per mole and on the other hand because it requires simulations of rather large systems often exceeding 100 atoms. This work is an attempt to complement experimental evidence in such systems with the results of quantum-mechanical simulations so as to gain a more complete understanding of an asymmetric catalytic reaction.

In earlier work by Togni et al.,[2,3] asymmetric allylic amination using a Pd catalyst containing ferrocenyl P,N-ligands as shown in Figure 1 has been investigated.

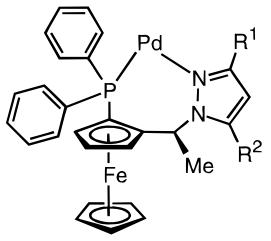

	R^1	R^2
(*S*)-(*R*)-**1**	1-Adamantyl	H
(*S*)-(*R*)-**2**	9-Anthryl	CH_3
(*S*)-(*R*)-**3**	Phenyl	CH_3
(*S*)-(*R*)-**4**	9-Triptycyl	H

Figure 1. Schematic diagram of the catalyst.

Typical selectivities for 1,3-diphenylallyl substrates in the range of 94−96% ee were obtained. However, the highest selectivity of 99% ee was obtained with catalyst **1**, containing a 1-adamantyl substituent. On the other hand, the very low value of 40% ee, yielding the opposite enantiomer, resulted from catalyst **2**. The bulky triptycyl group at the same position prohibited reaction at all. Another most useful aspect is the identification of various isomers of the allyl complexes and the determination of their relative concentrations for catalyst systems **1**−**4**. From our experiments, we concluded that the nucleophilic attack of the amine takes place at the allylic carbon trans to phosphorus.

While these experiments yield valuable information on the details of the reaction, a number of questions could not be answered conclusively. How important are steric and electronic effects for the selectivity of the reaction? What are the transition states? How can the concentrations of various isomers of the allyl complex

† IBM Research Division.
‡ Swiss Federal Institute of Technology.
⊗ Abstract published in *Advance ACS Abstracts,* August 15, 1996.

(1) Noyori, R. *Asymmetric Catalysis in Organic Synthesis*; Wiley: New York, 1994.
(2) Togni, A.; Burckhardt, U.; Gramlich, V.; Pregosin, P. S.; Salzmann, R. *J. Am. Chem. Soc.* **1996**, *118*, 1031.
(3) Burckhardt, U.; Gramlich, V.; Hoffmann, P.; Nesper, R.; Pregosin, P. S.; Salzmann, R.; Togni, A. *Organometallics* **1996**, *15*, 3496.
(4) Yoshida, S.; Sakaki, S.; Kobayashi, H. *Electronic Processes in Catalysis*; Verlag Chemie: Weinheim, Germany, 1994.

S0276-7333(96)00388-3 CCC: $12.00

Table 1. Bond Lengths in Å and Bond Angles in Degrees of the Model Allyl Complex As Compared with X-ray Structures of Related Compounds[a]

		exptl		
	model	**3**	**1**	**4**
d (Pd−C1)	2.147	2.141 (−0.3)	2.143 (−0.2)	2.160 (0.6)
d (Pd−C2)	2.158	2.173 (0.7)	2.188 (1.4)	2.062 (−4.4)
d (Pd−C3)	2.182	2.264 (3.8)	2.250 (3.1)	2.205 (1.1)
d (Pd−N1)	2.133	2.137 (0.2)	2.159 (1.2)	2.230 (4.5)
d (Pd−P)	2.364	2.319 (−1.9)	2.326 (−1.6)	2.353 (−0.5)
d (C1−C2)	1.421	1.440 (1.3)	1.440 (1.3)	1.386 (−2.5)
d (C2−C3)	1.409	1.383 (−1.8)	1.383 (−1.8)	1.365 (−3.1)
∠(P−Pd−N1)	90.8	95.1	95.3	101.1
∠(C1−C2−C3)	118.4	121.0	120.1	114.4
∠(P,N1,Pd)/(Pd,C1,C2)	26.8	12.0	9.1	20.7
∠(P,N1,Pd)/(Pd,C2,C3)	30.7	46.2	42.5	42.2

[a] See refs 2 and 3. C1 refers to the allyl carbon *cis* to P, N1 is the pyrazole nitrogen bound to Pd, C2 is the central allyl carbon, and C3 is the terminal allyl carbon trans to P. The numbers in parentheses are the percentage deviations from the model complex .

be related to the enantiomeric excess of the reaction? Here we attempt to answer these questions with the help of electronic structure calculations.

A related reaction, namely the nucleophilic attack of a Pd−allyl complex by a hydroxyl group, has been studied using semiempirical CNDO-type MO calculations.[4,5a] More recent work concerning nucleophilic attack on the central allylic carbon has been carried out by Mealli, Musco, and co-workers.[5b]

Our methods are first-principles electronic and atomic structure calculations using the projector augmented wave method,[12,13] an all-electron electronic structure method employing density functional theory[6,7] and first-principles molecular dynamics.[16]

In order to single out the electronic effects, we have studied model complexes that lack any steric hindrance but reproduce the electronic effects adequately. The steric effects are reproduced by calculations of the allyl complexes **1** and **3** using all side groups without approximations. The paper is organized as follows. (1) We investigate binding of the allyl to the Pd complex and discuss the structural asymmetry. (2) Then we discuss transition and final states for nucleophilic attack cis and trans to the phosphine with particular emphasis on the substrate rearrangement. (3) The influence of steric effects is investigated for the complex of the catalyst and the 1,3-diphenylallyl group, including all side groups. The resulting structures can be compared to the X-ray structures. (4) Finally, the interplay of steric and electronic effects will be elucidated, again on the model complexes, in which steric effects are emulated using external constraints.

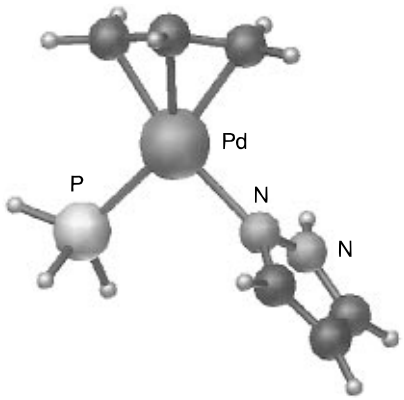

Figure 2. Front view of the allyl model complex.

2. Role of Electronic Effects

In order to separate out electronic effects on the site selectivity (*vide supra*), we have constructed a model system that lacks the steric hindrance present in the actual complex. The substituents of the allyl ligand have been removed, the chelating ligand has been replaced by phosphine (PH_3) and pyrazole, and the attacking amine is represented by simple ammonia. The rationale for these simplifications is to preserve the electronic structure of the ligand orbitals by cutting through single bonds and by saturating the created dangling bonds with hydrogen atoms, while removing as many side groups as possible. It should be noted that the phenyl groups of the allyl may participate in the delocalized π-electron clouds of the allyl. However, the comparison with the experimental X-ray structures indicates that this effect is of secondary importance. In this study we have only considered *exo*-oriented allyl ligands, that is, those with the C−H vector of the central allyl carbon pointing away from the ferrocene core.

A. The Pd(II)−Allyl Complex. The model complex between the negatively charged allyl and the Pd(II) catalyst, shown in Figure 2, is bonded so that the phosphine, the pyrazole ligand, and the two terminal carbon atoms of the allyl form an approximately square-planar arrangement around the Pd atom.

In Table 1, the structural data are compared with those from the X-ray crystal structures of the allyl complexes.[2] Throughout this paper, we use the following naming convention: C1 is the allyl carbon cis to the phosphine, C2 is the central allyl carbon, and C3 is the allyl carbon trans to the phosphine. By N1 we denote the pyrazole nitrogen atom binding to Pd, while N2 is

(5) (a) Sakaki, S.; Nishikawa, M.; Ohyoshi, A. *J. Am. Chem. Soc.* **1980**, *102*, 4062. (b) Carfagna, C.; Galarini, R.; Linn, K.; Lopez, J. A.; Mealli, C.; Musco, A. *Organometallics* **1993**, *12*, 3019.
(6) Hohenberg, P.; Kohn, W. *Phys. Rev. B* **1964**, *136*, 664.
(7) Kohn, W.; Sham, L. J. *Phys. Rev.* **1965**, *140*, B1133.
(8) Perdew, J. P.; Zunger, A. *Phys. Rev. B* **1981**, *23*, 5048.
(9) Perdew, J. P. *Phys. Rev. B* **1986**, *33*, 8822.
(10) Becke, A. D. *J. Chem. Phys.* **1992**, *96*, 2155.
(11) We hope that in the future such problems can be solved more efficiently by using either internal coordinates or another preconditioning scheme.
(12) Blöchl, P. E. *Phys. Rev. B* **1994**, *50*, 17953.
(13) Blöchl, P. E.; Margl, P.; Schwarz, K. In *Chemical Applications of Density-Functional Theory;* Laird, B. B., Ross, R. B., Ziegler, T., Eds.; ACS Symposium Series; American Chemical Society: Washington, DC, 1996; Vol. 629, p 54.
(14) Blöchl, P. E. *J. Chem. Phys.* **1995**, *103*, 7422.
(15) Margl, P.; Schwarz, K.; Blöchl, P. E. *J. Am. Chem. Soc.* **1994**, *116*, 11177.
(16) Car, R.; Parrinello, M. *Phys. Rev. Lett.* **1985**, *55*, 2471.

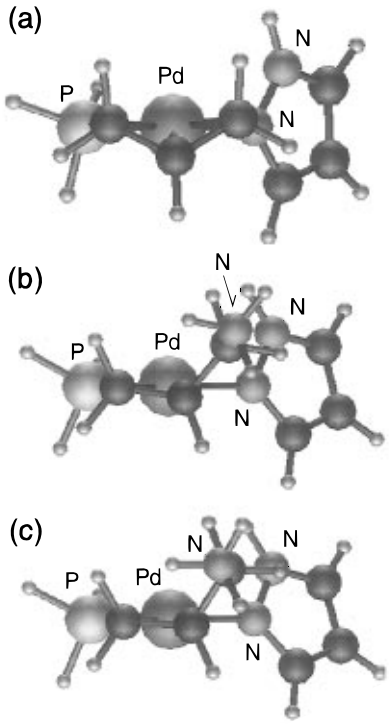

Figure 3. Top views of the allyl model complex: (a) allyl complex before the reaction, (b) transition state; (c) olefin complex.

the nitrogen atom of the attacking amine. The important structural data calculated for our model complex agree well with the X-ray structures. Bond lengths either lie between those measured for different catalysts or deviate by less than 1%. One notable exception is the C2−C3 bond length, which is about 2% larger in our model compound than in the X-ray structures. In contrast to the X-ray structures of the complete Pd−allyl complexes, however, no appreciable rotation of the allyl about the Pd−allyl axis is found. Figure 3a shows that there is only a slight rotation of the allyl group about the Pd−allyl axis.

The calculated structure exhibits a small asymmetry between the two terminal carbon atoms of the allyl, which distorts the allyl slightly toward a propene-like structure (prop-2-en-1-yl). This asymmetry of the allyl binding is visible from the slight elongation of the C1−C2 bond, as compared to the C2−C3 bond. The C1−C2 bond is longer than the C2−C3 bond by 4.1% in **1** and **3** and by 1.5% in **4**, while the asymmetry in our model complex is 0.9%. The asymmetry in the carbon bond lengths of the allyl is qualitatively similar to that of propene, where it is 12.3%.[17] Hence, the allyl in the complex is about 90% allyl-like and 10% propene-like. A bond-length asymmetry similar to that in propene is obtained in a calculation of 3-aminopropene, the product of the catalytic reaction, for which we find an asymmetry of 12.7%. Since the structural asymmetry is reproduced in our model—even though to a lesser extent than in the complete complexes—it must be attributed, at least partly, to electronic effects.

A second notable feature is a tilt of the allyl, such that the C3 is further removed from Pd than is C1. Again,

(17) *CRC Handbook of Chemistry and Physics*; Lide, D. R., Ed.; CRC Press: Boca Raton, FL, 1995.
(18) Rappe, A. K.; Casewitt, C. J.; Colwell, K. S.; Goddard, WA., III; Skiff, W. M. *J. Am. Chem. Soc.* **1993**, *114*, 10024.

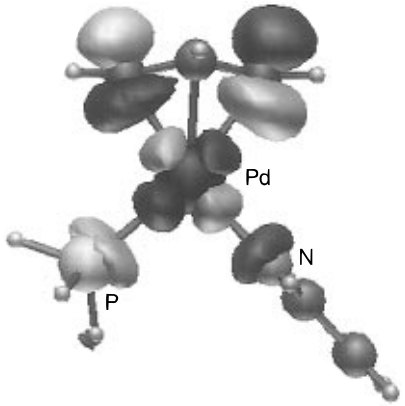

Figure 4. LUMO of the model allyl complex, the frontier orbital for nucleophilic attack.

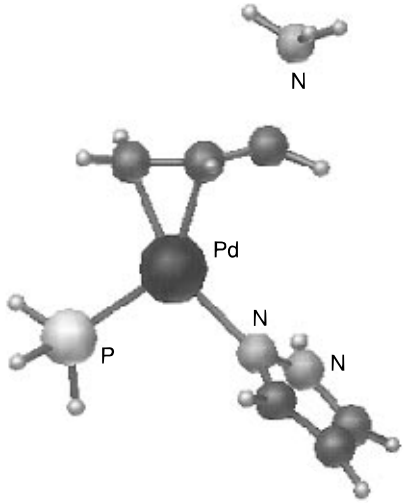

Figure 5. Transition state for nucleophilic addition in the model complex.

our model complex reproduces the effect, even though to a lesser extent than in the measured X-ray structures. If we express this tilt by the difference between the Pd−C3 bond length on the one hand and the Pd−C1 bond length on the other hand, we find a difference of 1.7% in our model compound, while the deviation in the X-ray structures is 6% for **3**, 5% for **1**, and 3% for **4**. We note that the two bond-length asymmetries are approximately linearly correlated for the different allyl complexes, which is an indication that they may have a common origin.

The asymmetry of the allyl complex may be explained by the stronger trans influence of phosphine. The electron density of the allyl is slightly more localized cis to the phosphine, which results in a tendency to establish a σ bond between C1 and Pd, while the remaining two carbon atoms, C2 and C3, strengthen their π-electron system.

From these results, one might expect that the labilization of the allylic carbon trans to the phosphine will in turn favor nucleophilic attack on that carbon. This conclusion is based on the assumption that the transition state for the reaction is similar to the Pd−allyl complex. Therefore, the transition state will be investigated next.

B. Nucleophilic Addition of an Amine to Allyl. Figure 4 shows the LUMO, which is the frontier orbital for nucleophilic attack. The orbital is the nonbonding

Table 2. Energetics of Nucleophilic Attack Cis and Trans to the Phosphine in the Unconstrained Model Complex[a]

	$E(d)$ trans to P	$E(d)$ cis to P
GA	0 (∞)	0 (∞)
TS	42 (1.884)	50 (1.932)
GO	36 (1.603)	41 (1.585)

[a] Energies in kJ/mol are given for the isolated ammonia molecule and the allyl complex GA, the transition state TS, and the olefin complex GO. Numbers in parentheses are the distances in Å between the amine nitrogen and the nearest allyl carbon atom.

Table 3. Bond Lengths in Å and Bond Angles and Angles between Planes in Degrees of the Transition State for Nucleophilic Attack and the Resulting Olefin Complex for Attack Cis and Trans to Phosphine[a]

	TS		GO	
quantity	trans to P	cis to P	trans to P	cis to P
d(Pd−C1)	2.082	2.751	2.071	3.054
d(Pd−C2)	2.147	2.133	2.121	2.097
d(Pd−C3)	2.806	2.101	3.031	2.095
d(Pd−N1)	2.187	2.158	2.190	2.173
d(Pd−P)	2.362	2.387	2.367	2.387
d(C1−C2)	1.437	1.433	1.441	1.486
d(C2−C3)	1.434	1.430	1.479	1.438
d(C1−N3)		1.932		1.585
d(C3−N3)	1.884		1.603	
∠(P−Pd−N1)	97.8	94.5	98.3	93.7
∠(C1−C2−C3)	122.8	122.2	121.2	120.5
∠(C2−C3−N3)	110.3		110.1	
∠(N3−C1−C2)		109.5		109.3
∠(P,N,Pd)/(Pd,C1,C2)	8.9	54.5	4.0	63.5
∠(P,N,Pd)/(Pd,C2,C3)	52.9	8.7	61.4	5.3

[a] TS refers to the transition state and GO to the ground state of the olefin complex. See Figure 2 or text for notation.

π-orbital of the allyl in an antibonding combination with a Pd orbital of type d_{xy}. This orbital has two pronounced lobes at the terminal carbon atoms C1 and C3 of the allyl. Hence, we investigated the transition states for amine addition at those two positions.

As the amine approaches the allyl complex, a double bond between C1 and C2 is formed and is attached in an η^2 mode to Pd. Furthermore, the allyl performs a translation along its long axis toward the attacking amine, combined with a rotation about the axis from the Pd atom to the center of the C1−C2 double bond, which aligns the double bond opposite to the amine with the P−Pd−N1 plane. In the transition states these movements have almost been completed. The activation energy for nucleophilic attack trans to P is 42 kJ/mol. The C3−N2 bond length in the transition state is 1.89 Å.

The calculated asymmetry in the activation energies for nucleophilic attack cis or trans to the phosphine ligand is 8 kJ/mol, as shown in Table 2. Note that 8 kJ/mol correspond to 92% ee at room temperature. This is in agreement with the typical selectivities obtained experimentally.

Interestingly, we obtain this asymmetry even though the bond in the transition state is olefinic rather than allylic. The asymmetry corresponds to an interchange of a hydrogen at C1 with the $CH_2\cdots NH_3$ fragment attached to C2. One would expect that the exchange of a σ bond to hydrogen with one to the $CH_2\cdots NH_3$ fragment will not affect the π-electron system, which is coupled to the Pd, and therefore the asymmetry should be small. However, as can be seen in Figure 6, there still is a substantial π-bond contribution for the latter fragment.

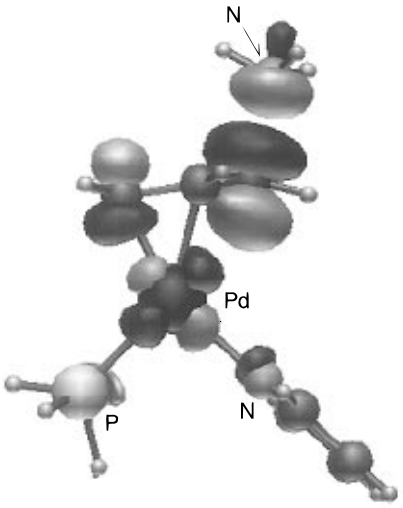

Figure 6. LUMO of the transition state for nucleophilic addition in the model complex.

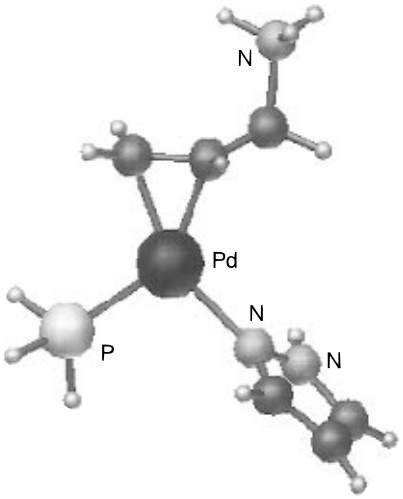

Figure 7. The olefin complex.

Even though the results discussed so far seem to indicate that the trans influence is the driving force behind the observed site selectivity, we will see later that the movements of the allyl group during nucleophilic attack are the main origin of site selectivity. As for the two competing pathways these movements go in opposite directions, steric hindrance can steer the reaction into one or the other direction by imposing the movements required to approach the transition state. This is exactly what happens for the complexes in which the steric interaction between the side groups forces the allyl into an orientation that is rotated out of the plane of the catalyst already before attack of a nucleophile.[2]

C. The Final State, a Pd(0)−Olefin Complex. Our calculations show that the Pd−olefin complex strongly resembles the transition state of the reaction. Furthermore, the barrier for the back-reaction is, at only 6 kJ/mol, small. The structure is shown in Figures 3 and 7.

Formally, the resulting complex corresponds to a Pd(0) configuration, with the positive charge located on the ammonium nitrogen atom. It may be somewhat surprising that a Pd(0) complex keeps a near-square-planar

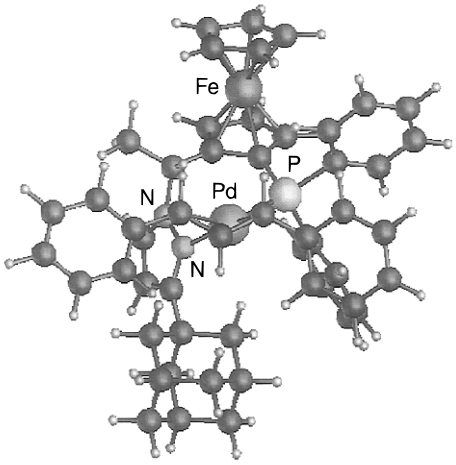

Figure 8. Top view of the complex between the allyl group and the catalyst with the adamantyl group. Note the rotation between the allyl and the N−Pd−P plane and the olefinic binding of only two carbons, thus freeing a valence on the third allylic carbon for amination.

configuration. For example, a Pd(0) model complex without allyl orients its ligands in mutually trans positions. This nondirectional bonding is expected because the d shell is filled, and the binding results mostly from the interaction between the filled ligand orbitals and the unoccupied metal s and p orbitals. In the olefin complex, however, the LUMO orbital still has considerable d character, which is sufficient to maintain the directional bonding of the d orbitals.

3. Interplay between Electronic and Steric Effects.

In order to account for steric effects, we have investigated the π-allyl complex of the substrate, and here all side groups are treated explicitly in our calculation. We have used catalyst **1**, which exhibits the largest selectivity, and **3**, which shows typical selectivities in the 95% range. For both complexes X-ray structures are available.[2] We performed *ab initio* molecular dynamics simulations at finite temperature of the catalyst allyl complex, starting from a configuration that has been prerelaxed using an interatomic force field. In the starting configuration of complex **1**, the allyl is already rotated as a consequence of the steric repulsions between the allyl and the adamantyl group as well as one phenyl group of the phosphine. While the interatomic force fields require predefined bonds, the *ab-initio* molecular dynamics simulation derives the forces from a quantum-mechanical description of the electronic structure in each time step and therefore accounts for bond formation. In this simulation, we observed that the allyl shifts spontaneously sideways and binds with two of its carbons, C1 and C2, to Pd. It thereby overcomes the steric hindrance of some hydrogen atoms of the adamantyl group, which are excited to vivid oscillations. Then the phenyl group attached to C3 starts a slight rotation, indicating an increased sp^3 character of the activated carbon. When we no longer observe any rearrangements of the side groups and the position of the allyl, we quench the system into the ground state.

The structural data of our calculations are summarized in Table 4 and compared to the X-ray structures. It should be noted that it has not been possible to reach full convergence. In order to obtain an estimate for the error bar for these large complexes, we have performed two calculations for the Pd−allyl complex. One was started as described above; the other was started from the X-ray structure. While most of the relevant calculated and measured structural parameters agree well, that is, within 1−2%, there are marked differences: First, the Pd−C3 bonds are 4−9% longer in **1** and 5% longer in **3** than those in the X-ray structures. Second, in our calculations the Pd−ligand bonds to the pyrazole are 2−3% and those to the phosphine 4.6% larger. Theory predicts a better alignment of the C1−C2 double bond with the P−Pd−N plane than what is found experimentally.

The main difference between the calculated structures for the Pd−allyl complex and the corresponding X-ray structure is a twist of the ligand, which causes the adamantyl group to push against the allyl ligand. This in turn is responsible for the large Pd−C3 distance compared to the experimental one. It is obvious that this degree of freedom is very hard to converge, because it is driven by bond torsions and involves the rearrangement of rather heavy side groups such as ferrocenyl and adamantyl.[11] The Pd−P bond length, however, is overestimated in all our calculations. There are two explanations for this discrepancy: it is due either to a deficiency of the density functional or to the lack of solvent and crystal-packing effects in our calculation. The surface pressure of a solvent, for example, could compress the complex, affecting the weakest bonds most and therefore contracting the Pd−C3 and Pd−P bonds.

Table 4. Calculated Bond Lengths in Å and Bond Angles and Angles between Planes in Degrees of the Allyl Complexes[a]

	complex **1**		complex **3**
d (Pd−C1)	2.152 (0.4)	2.170 (1.3)	2.158 (0.7)
d (Pd−C2)	2.202 (0.6)	2.194 (0.3)	2.185 (0.6)
d (Pd−C3)	2.453 (9.0)	2.340 (4.0)	2.387 (5.5)
d (Pd−N1)	2.198 (1.8)	2.204 (2.1)	2.181 (2.1)
d (Pd−P)	2.438 (4.8)	2.415 (3.8)	2.426 (4.6)
d (C1−C2)	1.443 (0.2)	1.436 (−0.3)	1.421 (0.0)
d (C2−C3)	1.397 (1.0)	1.401 (1.3)	1.399 (1.1)
∠(P−Pd−N1)	93.6 (−1.7)	96.3 (+1.0)	92.6 (−2.5)
∠(C1−C2−C3)	120.3 (0.2)	120.8 (0.7)	120.5 (−1.4)
∠(P,N,Pd)/(Pd,C1,C2)	4.2 (−5.1)	10.1 (1.0)	8.7 (−3.3)
∠(P,N,Pd)/(Pd,C2,C3)	55.4 (12.9)	43.6 (1.1)	53.5 (−7.3)

[a] All side groups of the complexes in the X-ray structures have been retained, except that the methyl group R^2 in **3** has been replaced by a hydrogen atom. The numbers in parentheses are the percentage deviations of the calculated values from those of the X-ray structures[2,3] as listed in Table 1. The numbers given in the second column of complex **1** have been obtained by starting by starting the relaxation from the crystal structure.

Table 5. Effect of the Orientation of the Allyl Group on the Activation Barriers[a]

	trans to P		cis to P	
	$z_{C3}-z_{C1}=1.21$	$z_{C3}-z_{C1}=-1.21$	$z_{C3}-z_{C1}=1.21$	$z_{C3}-z_{C1}=-1.21$
GA	21	20	21	20
TS	46	80	84	51
GO	36	78	81	41

[a] The energies of allyl complex GA, the transition state TS, and the olefin complex GO are given in kJ/mol. The orientation is prescribed by fixing the distance in the *z* direction (perpendicular to the P−Pd−N plane pointing into the exo direction) $z_{C3}-z_{C1}$ of the terminal allyl carbon atoms.

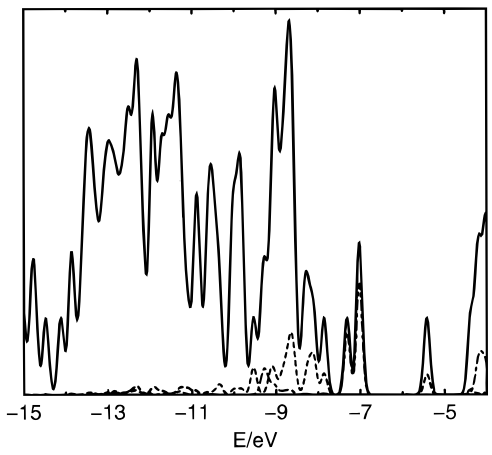

Figure 9. Density of states (DOS) of the allyl complex (solid line). Pd-projected DOS (dashed line) and Fe-projected DOS (dash-dotted line). Dashed and solid lines almost overlay each other at the double peak at −7 eV. The DOS is broadened with a Gaussian of 0.1 eV half-width.

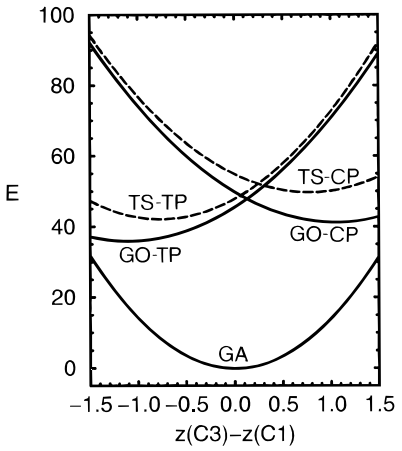

Figure 10. Energies of the allyl model complex GA in kJ/mol, the transition state TS and the olefin complex GO depending on the out-of-plane orientation of the long axis of the allyl. CP and TP denote the energies for nucleophilic attack cis and trans to the phosphine.

The density of states of the allyl complex **1** is shown in Figure 9. The state at $E = -5.5$ eV is the LUMO, the frontier orbital for nucleophilic attack by the amine. This state corresponds to that shown in Figure 4 for the model complex. Interestingly, the HOMO is a member of a group of three states with Fe d character at −7.3 to −7.0 eV. The occupied Pd states are located below −7.7 eV.

4. Effect of the Enforced Rotation on the Transition State

Here, we investigate the effect the allyl rotation has on the reaction pathway. We return to our model complex but now mimic the steric effects by an external constraint prescribing the orientation of the C1−C3 axis out of the P−Pd−N plane. We choose the values such that either the C1−C2 or the C2−C3 bond is approximately parallel to the P−Pd−N plane. We have limited our study to nucleophilic attack at C3 but considered both constraints that rotate the allyl into opposite directions.

For the allyl complexes we observe that the constraints increase the bond-length asymmetries to approximately twice the value obtained without constraints, when C3 is rotated out of the plane of the catalyst, bringing these results into better agreement with the X-ray structures. While the orientation changes, the allyl in the transition state rotates about the axis connecting the center of the double bond with Pd.

The activation barriers for nucleophilic attack at C1 as compared to C3 differ by about as much as 30 kJ/mol (see Figure 10). Hence, the enantiomeric excess resulting from a given isomer of the allyl complex approaches 100%. This indicates that the binding of the allyl to the catalyst already determines the handedness of the product. Furthermore, the enforced rotation reduces the barrier, owing to the destabilization of the Pd−allyl complex before the reaction. Fluctuations can change the orientation of the allyl and therefore modulate the resulting enantiomeric excess. The difference in the activation energies varies approximately linearly with the out-of-plane angle, vanishing if the long axis of the allyl is aligned with the plane of the catalyst. The same fluctuations also increase the barrier by "stabilizing" the allyl complex.

5. Discussion

We conclude that the high enantioselectivities result from an interplay of electronic and steric effects. Electronic effects are only partially related to the trans influence of the phosphine.

If one terminal carbon of the allyl is attacked by a nucleophile, the other terminal carbon forms a double bond with the central carbon (C2), which strongly prefers alignment with the P−Pd−N1 plane. This implies that at the transition state the long-axis allyl is rotated out of the natural plane of the catalyst and the allyl is rotated in an opposite direction, depending on the site at which nucleophilic attack occurs.

Correspondingly, if steric interactions force the allyl into an orientation rotated out of the natural plane of the catalyst, the transition state for nucleophilic attack at one terminal carbon is stabilized, while the other one is destabilized. This causes, for a given orientation, a difference between the activation energies cis or trans to phosphine of about 30 kJ/mol, making the reaction almost 100% site selective. These steric effects are caused by a groove in the catalyst surface that forces the natural axis of the allyl to align at a certain angle to the natural plane of the transition-metal center. Hence, the trans influence is not the dominant effect for selectivity, and steric effects determine the course of the reaction in an indirect way.

The selectivity is closely related to the stability of the various isomers of the 1,3-diphenylallyl complex. Six such isomers have to be considered. They are the *exo-syn-syn*, *exo-syn-anti*, *exo-anti-syn*, *endo-syn-syn*, *endo-syn-anti*; and *endo-anti-syn* isomers shown in Figure 11. *syn* and *anti* define the orientation of the phenyl groups at the terminal allyl carbon atom, which points along the C2−C3 bond for *syn* and perpendicular to it for *anti*. The first *syn* or *anti* refers to the carbon atom C1 cis to the phosphine and the second to the carbon atom C3 trans to the phosphine. We do not consider *anti-anti* isomers because of the unfavorable interaction of the two phenyl groups, which forces them to rotate out of the plane of the allyl carbons.

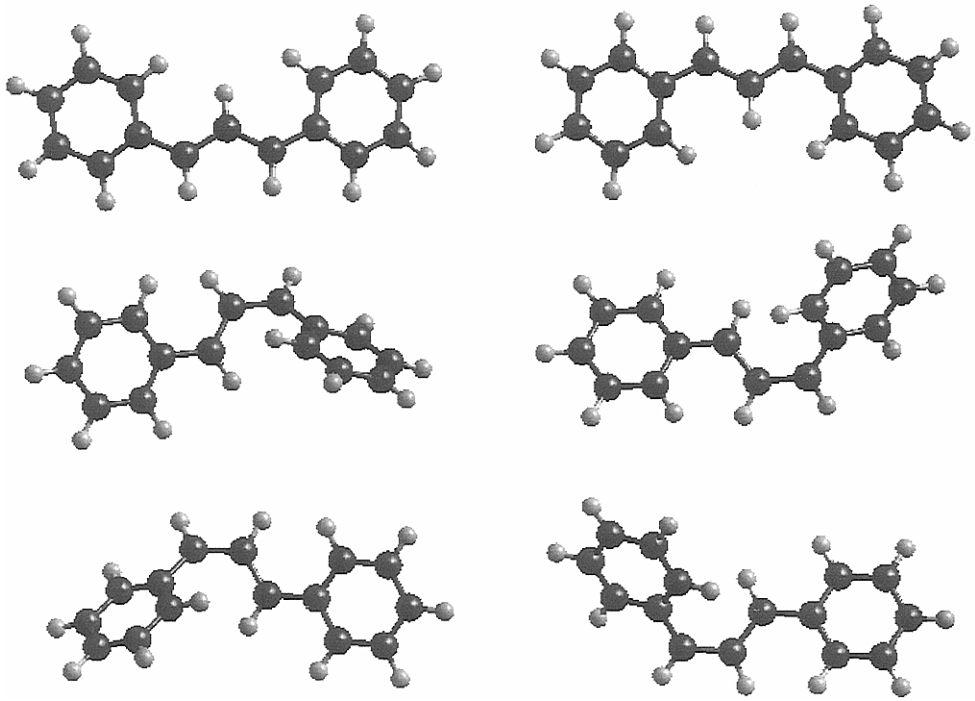

Figure 11. Six isomers of the 1,3-diphenylallyl complex. The groove of the catalyst is oriented horizontally, and the plane of the transition-metal center would be rotated by 45° out of the plane with the nitrogen ligand right above the phosphine ligand with the ferrocenyl below the allyl.

Let us now extrapolate our findings to the six different isomers shown in Figure 11. We deduce the rule that for each of the isomers C3 is the site for nucleophilic attack, if the C1−C2 bond exhibits a better alignment to the P−Pd−N1 than to the C2−C3 plane. Otherwise, C1 is the reactive site. Thus, for ligands with the *S*,*R* absolute configuration, as shown in Figure 1, we expect that four isomers react to form (*R*)-1-amino-1,3-diphenylprop-2-ene: the *exo-syn-syn*, *exo-anti-syn*, *endo-syn-syn*, and *endo-syn-anti* isomers. The remaining two isomers, namely the *exo-syn-anti* and *endo-anti-syn*, react to the corresponding (*S*)-aminopropene. If nucleophilic attack always occurred trans to phosphine, the *endo-syn-syn* isomer would react to give a different isomer, namely the *S* isomer.

We believe that state-of-the-art electronic structure calculations are not yet able to predict the relative stabilities of the isomers with sufficient accuracy, in particular because they do not yet take solvent effects into account.

However, we shall see that our predictions together with measured concentrations of the isomers can be related to the selectivity of the catalytic reaction. In this discussion we assume that the product distribution is correlated directly to the distribution of the various isomers. This assumption is supported by the experiments discussed below and implies that (1) the activation energy for nucleophilic attack is similar for all isomers and (2) the transition state for dissociation of 1-aminopropene from Pd(0) is lower than the barrier for nucleophilic attack.

We first discuss the isomeric distribution of the complex with **2**. Here, 71% of the *exo-syn-anti* and 29% of the *exo-syn-syn* complex have been observed.[2] Both isomers react at C3, irrespective of whether we apply the rule of attack trans to phosphine or our new rule. This experiment cannot differentiate between the two prescriptions but clearly shows a direct link between the isomeric distribution and the enantioselectivity of 42% *S* of the reaction.

For catalyst **3** the following concentrations of the various isomers have been observed:[2,3] 85% of the *exo-syn-syn* isomer, 6% of the *endo-syn-syn* isomer, 6% of the *endo-syn-anti* isomer, and 3% of some unidentified isomer. The product had 96% ee. This result could not be understood simply from the rule that nucleophilic attack always takes place trans to the phosphine, because then at least the *endo-syn-syn* conformer should result in the wrong product, thus limiting selectivity to less than 70−76% ee. From our interpretation, we predict a different handedness of the product resulting from the *endo-syn-syn* isomer, which increases the anticipated enantiomeric excess by 12% to 82−88% ee. The remaining discrepancy indicates that the activation barriers are not strictly identical for all isomers. This effect could be caused by a less strong alignment of the allyl for the *endo-syn-anti* isomer, which would decrease the barrier by "stabilizing" the allyl complex owing to reduced steric interactions.

So far we have based our discussion on calculations in a vacuum. Now we wish to mention the possible role of solvent effects. The reactions have been performed in THF. (1) The barrier for nucleophilic attack is expected to be underestimated in our calculations, because THF itself is a weak nucleophile and may partially saturate the reactive sites of the allyl complex. Hence, before the amine can form a bond with the allyl, it has to displace a solvent molecule first. (2) The barrier for dissociation of aminopropene from the catalyst is severely overestimated in a vacuum calculation, because it involves charge separation, which is facilitated in a screening environment. (3) The aminopropene exposes the charge of the complex better to the solvent and may allow better screening, thus stabilizing the aminopropene complex compared to the allyl complex.

6. Computational Details

The calculations are based on the density functional theory as parameterized by Perdew and Zunger,[8] with Becke's gradient corrections for exchange[10] and Perdew's gradient correction for correlation.[9]

All calculations have been performed with the projector augmented wave (PAW) method.[12,13] The PAW method is an all-electron method that divides the valence wave functions into a plane wave expansion and two one-center expansions per atom, expressed by radial functions times spherical harmonics. The core electrons are treated in the frozen-core approximation. The plane-wave part of the wave functions has been expanded up to a kinetic energy cutoff of 30 Ry and that of the density up to 60 Ry.

All calculations on the model complexes have been performed in a face-centered orthorhombic supercell with lattice constants (in Å) of (7.5, 0, 9.5), (7.5, 0, −9.5), and (0, 14, 0) except for the isolated compounds. For the model compounds, we have fixed the three translational and the three rotational degrees of freedom by constraints that fix the Pd atom at the origin: two that keep the phosphorus on the line (s, $-s$, 0) and one that fixes the nitrogen ligand in the $z = 0$ plane. These constraints allow all internal relaxations of the molecules but orient the complexes in a well-defined way. For all other cases we have used fcc supercells, and in all cases the minimum distance between periodic images has been 6 Å or more. The full complex has been calculated in an fcc supercell with a lattice constant of 29 Å.

All calculations have been performed in the fashion of *ab initio* molecular dynamics;[16] that is, a dynamic equation is solved for both electron and nuclear dynamics. We use friction dynamics to find ground states, and convergence is checked by simulating with zero friction. The simulations have been performed with a time step of 20 au = 0.48 fs. We have used an electronic mass that explicitly depends on the **G** vector and can be expressed as $m_\Psi(G)$ (au) $= 1000(1 + {}^1/_2G^2)$.

Periodic images, which are automatically created in a plane-wave-derived basis set, have been electrostatically decoupled from each other by a mapping to a point charge model and Ewald summations,[14] using three decay lengths, with values of 0.5, 0.75, and 1.0125 for the Gaussians used in the charge density/potential fit and a weight function that cuts off the plane-wave contribution beyond a kinetic energy cutoff of 3 Ry.

Transition states are obtained in the following way. The C−N bond length is constrained to a certain value. Next, the electronic and the atomic structures are optimized until the total energy is minimized. Then the procedure is repeated for different values of the bond length. The configuration with the highest energy obtained in this way is the transition state separating two (meta-) stable configurations. This procedure converges at a saddle point of the total energy surface of first order, that is, with exactly one eigenmode with negative curvature. (1) It is fairly obvious that the gradient at the resulting configuration vanishes, because we maximize the total energy parallel to the force of constraint and minimize it perpendicular to the force. (2) To show that the state obtained has exactly one direction with negative curvature is slightly more involved but can be shown as follows: near the saddle point, we expand the total energy as $E(R) = E_{TS} + {}^1/_2\vec{R}D\vec{R}$, where $\vec{R}$ is the $3N$-dimensional vector describing the atomic positions relative to the transition-state configuration. E_{TS} is the energy of the transition state, and D is the matrix of second derivatives of the total energy. Near the transition state the constraint can be linearized as $\vec{c}\vec{R} = a$. Let us now assume that there were two or more negative eigenvalues of the dynamic matrix. In this case we can always form a combination of the vectors with negative eigenvalues that is perpendicular to $\vec{c}$. As our procedure always searches in all directions perpendicular to $\vec{c}$ for the lowest energy, it would follow such a direction away from the "transition state" and therefore would not converge. This proves that there will be at most one eigenmode with negative curvature if the procedure converges. As the system is unstable for distortions along the reaction coordinate $\vec{c}$, there is exactly one such mode.

All calculations are spin-restricted, because (1) ESR measurements excluded the presence of unpaired spins and (2) one spin-unrestricted calculation of the model complex in the final state of the nucleophilic attack, for which spin polarization would be most likely, showed no spin density.

OM9603880